Numerical Solutions for the Shape-Preserving Two-Dimensional Thermal Convection Element

DOUGLAS K. LILLY

U. S. Weather Bureau, General Circulation Research Laboratory

(Manuscript received 23 April 1963, in revised form 23 October 1963)

ABSTRACT

The convective motions developed upon release of a line of fluid into a large body of miscible homogeneous fluid of a different density have been previously investigated experimentally by J. M. Richards and found to be approximately shape-preserving. To investigate this phenomenon theoretically, the two-dimensional ($x-z$) Boussinesq equations are here subjected to a space-time transformation such that shape-preserving buoyant elements (thermals) are steady state solutions in the transformed variables. Such solutions are approached asymptotically, for various values of spatially constant eddy viscosity and diffusion coefficients, by numerical time integration of a finite difference analog from given initial conditions. The solution for one set of coefficients is found to correspond rather closely with laboratory data obtained from Richards, while those for lower diffusion coefficients tend toward formation of a separated vortex pair. Solutions obtained by varying the eddy Prandtl number exhibit complex behavior. The effects of the finite boundary approximations used are found generally negligible except for the low diffusion cases. The transient behavior helps relate the steady-state results to numerical solutions of transient behavior previously presented by Lilly and Ogura. The finite difference scheme used, adopted from work of A. Arakawa, conserves integrated momentum and quantities analogous to total energy and temperature variance.

1. Introduction

When a parcel or horizontal line of fluid is released in a homogeneous motionless mass of miscible denser (or lighter) fluid, it tends to develop a circulating vortex structure and increases in size as it rises (or falls) through the ambient fluid. Provided that the ratio of densities of the parcel and ambient fluid is not far from unity and the Rayleigh number is sufficiently large, experiments show that an approximately shape-preserving flow pattern is generated and maintained until the identifiable element reaches the upper (lower) boundary of the homogeneous fluid. Fig. 1, taken from Richards (1963a) illustrates a typical form of the resultant "thermal" or, as it is here designated, buoyant element.

Scorer and Ludlam (1953) were among the first to recognize the phenomenon as related to some of the visible aspects of atmospheric convection. Batchelor (1954), Levine (1959), Malkus and Witt (1959), Morton, Taylor and Turner (1956), Ogura (1962), Saunders (1961), Scorer (1957), Richards (1963a), Woodward (1959) and others have contributed theoretical, observational and experimental efforts toward description and understanding of its nature. Besides the apparent application to meteorology, recent theoretical results by Kuo (1961) suggest that convection patterns in heated parallel plate experiments may also be closely related to isolated buoyant elements. Scorer (1959) has also suggested applications of the laboratory and theoretical results toward the design and performance of smokestacks.

Using the assumption that the rising and expanding buoyant element develops and maintains a constant shape, Batchelor, Scorer, and others have applied dimensional analysis to show that the characteristic length, velocity and buoyancy must be related to certain powers of time for both the line symmetric (line source) and axially symmetric (point source) elements. For the axial case, in which the characteristic Rayleigh and

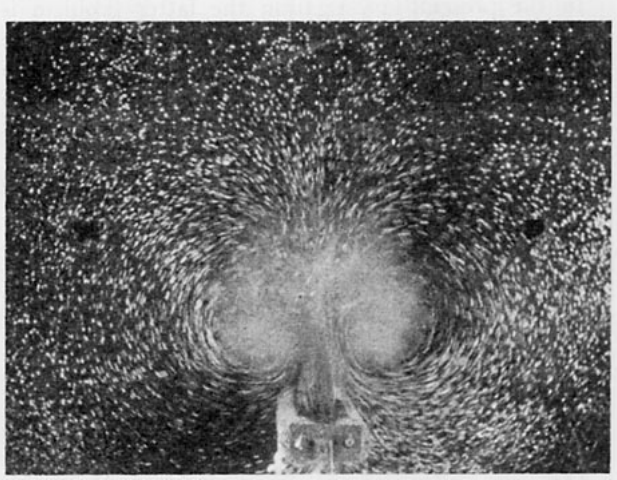

FIG. 1. Short time exposure of a secton of a two-dimensional buoyant fluid element. The streaks are trajectories of tracer particles (Photo from J. M. Richards).

Reynolds numbers are constant with time, Morton (1960) has exhibited a quasi-nonlinear series solution, valid for infinite boundary conditions and Rayleigh numbers of up to 10 or more. Numerical time integrations of the basic governing equations in two dimensions, carried out by Malkus and Witt (1959), Lilly (1962) and Ogura (1962) have shown that, with large or infinite Rayleigh number, the simulated motion and thermal fields tend toward the shape-preserving patterns.

The results of previous numerical computations were, however, difficult to compare either with each other or with observations because of difficulties and inconsistencies in the numerical formulations. Those obtained by Malkus and Witt were limited to the initial stage of accelerating growth because of the development of nonlinear computational instability. Ogura avoided this difficulty by using an uncentered space and time integration scheme (the "upwind" difference scheme), but at the cost of considerable loss of conservation of mass and energy. Lilly used centered-difference conservation equations, with a variable viscosity formulation intended to simulate eddy transfers in an inertial subrange of turbulence. The difficulty encountered here was a little more subtle, although equally serious, and apparently involved the impossibility of developing an inertial sub-range in a two-dimensional fluid. In addition, and most important in motivating the present work, results of the latter two investigations were severely constrained by presence of a rigid upper boundary.

In order to reach the shape-preserving regime from arbitrary initial conditions it is apparently necessary to allow growth of the buoyant element to at least 10–20 times its initial size before it reaches a boundary. The previous computations were not performed with a sufficient number of mesh points to allow this development, and it would seem hardly worth the computational effort to do so.

In the present investigation the latter problem is overcome by allowing the spatial coordinates of the mesh points and boundaries to stretch with time in such a way that a shape-preserving solution in absolute coordinates becomes a steady-state solution in the new stretched coordinates. It is later shown that the existence of such a solution implies that eddy diffusivity must be non-zero and, that if coefficients of eddy viscosity and diffusion are defined, their variation with time is prescribed by the coordinate transformation. In the calculations described here spatial variation of these parameters is not allowed and they are set constant in the dimensionless stretched-coordinate equations. This form of mixing length assumption is far from the best available, and is in a sense a retrogression from previous related work. It was applied originally as a first crude approximation, to be improved upon in subsequent calculations. The results, as presented in this paper, appear to represent the phenomenon sufficiently accurately, however, that there seems little point in refining the method. The remaining physical misrepresentations are probably most closely connected with elimination of three-dimensional motions.

The steady state solutions are approached asymptotically by numerical integration of time-dependent equations from stationary initial conditions. The use of this method insures that, if a steady-state solution is obtained, it is stable to small perturbations. There may, perhaps, be other equally stable solutions which are not approachable from the initial conditions used, but several trials suggest that this is unlikely for the range of viscosity and diffusion used here.

It has become abundantly clear, in recent years, that moist atmospheric convective motions are much more complex than those in a simple buoyant element, and thus even a very complete explanation of the dynamics of the latter will only give partial clues to those of the former. The laboratory results represent, however, the best available sources of verifying data, and it was felt that an attempt at simulation of these would help determine the degree of success which might be expected from the use of similar methods in dealing with less verifiable natural phenomena.

2. Governing equations and numerical solution methods

We consider a semi-infinite incompressible fluid for which the Boussinesq approximations are valid. The equations of motion, continuity, and heat may be written in two-dimensional Cartesian coordinates as follows:

$$\frac{\partial u}{\partial t}=-u\frac{\partial u}{\partial x}-w\frac{\partial u}{\partial z}-\frac{\partial \pi}{\partial x}+\nu\nabla^2 u \tag{2.1}$$

$$\frac{\partial w}{\partial t}=-u\frac{\partial w}{\partial x}-w\frac{\partial w}{\partial z}-\frac{\partial \pi}{\partial z}+g\alpha(T-T_0)+\nu\nabla^2 w \tag{2.2}$$

$$\frac{\partial u}{\partial x}+\frac{\partial w}{\partial z}=0 \tag{2.3}$$

$$\frac{\partial T}{\partial t}=-u\frac{\partial T}{\partial x}-w\frac{\partial T}{\partial z}+\kappa\nabla^2 T \tag{2.4}$$

where u and w are the horizontal and vertical velocity components, T the temperature deviation from an arbitrary reference temperature T_0, g the acceleration of gravity, α the thermal expansion coefficient, and ν and κ are assumed *eddy* kinematic viscosity and diffusion coefficients, respectively. The pressure variable is $\pi=p/\bar{\rho}$, where p is the pressure deviation from a base hydrostatic field, and $\bar{\rho}$ is the mean density.

We wish to find a solution corresponding to a parcel of heated fluid released from a lower boundary. We

assume rigid free-slip insulated conditions at the lower boundary, i.e.,

$$\left.\begin{aligned} w&=0 \\ \frac{\partial u}{\partial z}&=0 \\ \frac{\partial T}{\partial z}&=0 \end{aligned}\right\} \quad \text{at} \quad z=0 \qquad \begin{aligned}&(2.5a)\\&(2.5b)\\&(2.5c)\end{aligned}$$

and the vanishing of u, w, and T, etc., as x and z approach infinity. Condition (2.5b) could be replaced by a non-slip condition ($u=0$). For a parcel released in a fully infinite fluid (2.5) would be replaced by vanishing amplitudes as $|z|\to\infty$. Modification of the infinite boundary conditions will be discussed in a later paragraph. We also assume reflective conditions on the left boundary, so that this boundary actually represents a symmetry line dividing the element in half. These are:

$$\left.\begin{aligned} u&=0 \\ \frac{\partial w}{\partial x}&=0 \\ \frac{\partial T}{\partial x}&=0 \end{aligned}\right\} \quad \text{at} \quad x=0. \qquad \begin{aligned}&(2.6a)\\&(2.6b)\\&(2.6c)\end{aligned}$$

Because of the two-dimensionality and incompressibility a stream function ψ may be defined such that

$$u=-\frac{\partial\psi}{\partial z}, \quad w=\frac{\partial\psi}{\partial x} \tag{2.7}$$

$$\eta=\frac{\partial u}{\partial z}-\frac{\partial w}{\partial x}=\nabla^2\psi \tag{2.8}$$

where η is the vorticity. A vorticity equation is obtained by differentiating (2.1) and (2.2) to eliminate π:

$$\frac{\partial\eta}{\partial t}=-\frac{\partial}{\partial x}(u\eta)-\frac{\partial}{\partial z}(w\eta)-g\alpha\frac{\partial T}{\partial x}+\nu\nabla^2\eta. \tag{2.9}$$

Boundary conditions (2.5a), (2.5b) and (2.6a), (2.6b) may be written as:

$$\eta=\psi=0 \quad \text{at} \quad x=0 \tag{2.10}$$

$$\eta=\psi=0 \quad \text{at} \quad z=0. \tag{2.11}$$

We now proceed to transform the above equations written in an inertial reference frame into a non-dimensional form which will define the requirements for attaining the shape similarity regime. Upon introduction of length and temperature scales, L and Θ, respectively, both to be functions of time alone, we now define dimensionless variables as follows:

$$\begin{gathered} x'=\frac{x}{L}, \quad z'=\frac{z}{L}, \quad T'=\frac{T-T_0}{\Theta}, \\ u'=\frac{u}{\dot L}, \quad w'=\frac{w}{\dot L}, \quad \pi'=\frac{\pi}{\dot L^2}, \quad \psi'=\frac{\psi}{L\dot L} \end{gathered} \tag{2.12}$$

where the dot operator signifies time differentiation. Then, upon recognition of the differentiation rules

$$\begin{aligned} \frac{d}{dt}&=\frac{\partial}{\partial t}\Big|_{x',z'}+\frac{dx'}{dt}\frac{\partial}{\partial x'}+\frac{dz'}{dt}\frac{\partial}{\partial z'} \\ &=\frac{\partial}{\partial t}\Big|_{x',z'}+\frac{\dot L}{L}\left[(u'-x')\frac{\partial}{\partial x'}+(w'-z')\frac{\partial}{\partial z'}\right] \end{aligned} \tag{2.13}$$

equations (2.1)–(2.4) may be written:

$$\frac{L}{\dot L}\frac{\partial u'}{\partial t}\Big|_{x',z'}=-\frac{L\ddot L}{\dot L^2}u'-\left[(u'-x')\frac{\partial u'}{\partial x'}+(w'-z')\frac{\partial u'}{\partial z'}\right]-\frac{\partial\pi'}{\partial x'}+\nu'\nabla'^2u' \tag{2.14}$$

$$\frac{L}{\dot L}\frac{\partial w'}{\partial t}\Big|_{x',z'}=-\frac{L\ddot L}{\dot L^2}w'-\left[(u'-x')\frac{\partial w'}{\partial x'}+(w'-z')\frac{\partial w'}{\partial z'}\right]-\frac{\partial\pi'}{\partial z'}-\frac{Lg\alpha\Theta}{\dot L^2}T'+\nu'\nabla'^2w' \tag{2.15}$$

$$\frac{\partial u'}{\partial x'}+\frac{\partial w'}{\partial z'}=0 \tag{2.16}$$

$$\frac{L}{\dot L}\frac{\partial T'}{\partial t}\Big|_{x',z'}=-\left(\frac{L}{\dot L}\frac{\dot\Theta}{\Theta}+2\right)T'-\frac{\partial}{\partial x'}[(u'-x')T']-\frac{\partial}{\partial z'}[(w'-z')T']+\kappa'\nabla'^2T' \tag{2.17}$$

where we have also introduced the new quantities

$$\nu'=\frac{\nu}{L\dot L}, \quad \kappa'=\frac{\kappa}{L\dot L}, \quad \nabla'^2=\frac{\partial^2}{\partial x'^2}+\frac{\partial^2}{\partial z'^2}. \tag{2.18}$$

The equations are now dimensionless except in the time derivatives. In order to simplify those terms and determine relationships between the scaling quantities we impose the following physical requirements on the system: a) all terms remain of the same order in time and of comparable order of magnitude; b) the total integrated temperature, i.e., total buoyancy, remain constant with time; and c) all velocities and disturbance quantities vanish as $|x'|$ and $z'\to\infty$. Upon spatial

integration of (2.17) and application of requirements b) and c) we see that the first term on the right must vanish, and therefore that

$$\Theta L^2 = \text{constant} = Q. \tag{2.19a}$$

If the buoyancy force term of (2.15) is to be of the same order as the others in that equation, then the coefficient

$$\frac{L}{\dot{L}^2} g\alpha\Theta = \text{constant}. \tag{2.19b}$$

We define the constant Q of (2.19a) to be $1/(2g\alpha)$ times the total buoyancy per unit length of the element and set the dimensionless constant of (2.19b) equal to unity. Upon solving (2.19a), and (2.19b) for the time dependence we then obtain

$$\frac{L}{L_0} = \left(\frac{t}{t_0}\right)^{2/3}, \quad \frac{\Theta}{\Theta_0} = \left(\frac{t}{t_0}\right)^{-4/3} \tag{2.20}$$

where t_0, Θ_0, and L_0 are initial values, related by the expressions

$$\Theta_0 = \frac{Q}{L_0^2}, \quad t_0 = \frac{2}{3}\left(\frac{L_0^3}{g\alpha Q}\right)^{1/2} \tag{2.21}$$

in which L_0 and Q have been considered to be the fundamental physical parameters. The interpretation of L_0 and Θ_0 depends somewhat on the initial conditions chosen, but if these consisted of a finite area of constant temperature excess, L_0^2 would be the area and Θ_0 the temperature excess. From substitution of these relations into (2.12) we obtain scaling quantities for the dependent and independent variables as follows:

$$\begin{Bmatrix} u \\ w \end{Bmatrix} = \frac{2}{3}\left(\frac{g\alpha Q}{t}\right)^{\frac{1}{3}} \begin{Bmatrix} u'(x',z',t') \\ w'(x',z',t') \end{Bmatrix} \tag{2.22a}$$

$$T - T_0 = \frac{Q}{[(9/4)g\alpha Q t^2]^{\frac{1}{3}}} T'(x',z',t') \tag{2.22b}$$

$$\begin{Bmatrix} x \\ z \end{Bmatrix} = \left(\frac{9}{4} g\alpha Q t^2\right)^{\frac{1}{3}} \begin{Bmatrix} x' \\ z' \end{Bmatrix} \tag{2.22c}$$

$$t = \frac{4}{9}\left(\frac{L_0^3}{g\alpha Q}\right)^{\frac{1}{3}} t'. \tag{2.22d}$$

The length parameter L_0 only appears in the t' dependence of the primed variables, [see equation (2.22d)] so that a steady state solution of u', w' and T' is a function only of the parameter Q. Such a solution is obviously shape-preserving in x-z space, since both spatial dimensions are scaled by the same factor.

We note that if shape-preserving solutions are to include diffusive effects ν' and κ' must be constant, and therefore, from (2.18), ν and $\kappa \propto L\dot{L}$, the product of characteristic spatial and velocity scales. This result could be obtained equally well from a mixing length argument.

We now apply the above relations to (2.14)–(2.17) and rewrite them, dropping the primes for convenience:

$$\frac{\partial u}{\partial s} = \frac{u}{2} - (u-x)\frac{\partial u}{\partial x} - (w-z)\frac{\partial u}{\partial z} - \frac{\partial \pi}{\partial x} + \nu\nabla^2 u \tag{2.23}$$

$$\frac{\partial w}{\partial s} = \frac{w}{2} - (u-x)\frac{\partial w}{\partial x} - (w-z)\frac{\partial w}{\partial z} - \frac{\partial \pi}{\partial z} + T + \nu\nabla^2 w \tag{2.24}$$

$$\frac{\partial u}{\partial x} + \frac{\partial w}{\partial z} = 0 \tag{2.25}$$

$$\frac{\partial T}{\partial s} = -\frac{\partial}{\partial x}[(u-x)T] - \frac{\partial}{\partial z}[(w-z)T] + \kappa\nabla^2 T. \tag{2.26}$$

The new time variable s is now defined as

$$s = \tfrac{2}{3} \ln\left(\frac{t}{t_0}\right). \tag{2.27}$$

The vorticity equation written in the transformed variables becomes:

$$\frac{\partial \eta}{\partial s} = \frac{\eta}{2} - \frac{\partial}{\partial x}[(u-x)\eta] - \frac{\partial}{\partial z}[(w-z)\eta] - \frac{\partial T}{\partial x} + \nu\nabla^2\eta \tag{2.28}$$

while boundary conditions (2.5), (2.6), (2.10) and (2.11) remain unchanged by the transformation.

The infinite boundary conditions on velocity and temperature are sufficient to determine a complete solution of our system in space and time, given suitable initial conditions. Since we are concerned with obtaining a numerical solution, however, we confine attention to a limited area of the transformed space in which it is hoped that the major portion of the energetics takes place and we replace the infinite boundary conditions by (2.5) and (2.6) at $z=H$, $x=D$, respectively, where H and D are the boundary locations in dimensionless coordinates. Since it is difficult to place any reasonable physical interpretation on these outer boundary conditions some effort was expended in evaluating the errors caused by their application. A further analysis will be presented in Appendix 2.

The final transformation of the governing equations will consist of the replacement of the continuous differential system by its finite difference analog. To facilitate a compact display we define the following sum and difference operators, in a notation similar to that of Shuman (1962):

$$\delta_\xi\varphi=\frac{\varphi\left(\xi+\frac{\Delta\xi}{2}\right)-\varphi\left(\xi-\frac{\Delta\xi}{2}\right)}{\Delta\xi}, \qquad (2.29)$$

$$\bar{\varphi}^\xi=\frac{\varphi\left(\xi+\frac{\Delta\xi}{2}\right)+\varphi\left(\xi-\frac{\Delta\xi}{2}\right)}{2}$$

where φ is any function of any discrete variable ξ, and $\Delta\xi$ is the discrete interval of ξ. We now locate ψ and T at mesh points of a square net in dimensionless x-z space (thus $\Delta x=\Delta z=\Delta$) and at times $m\Delta s$, where m is the time index (an integer). The velocities will be defined by the relations

$$u=\delta_z\psi, \quad w=-\delta_x\psi \qquad (2.30)$$

thus satisfying the finite difference analog of (2.25)

$$\delta_x u+\delta_z w=0 \qquad (2.31)$$

at points intermediate to those where ψ and T are defined. Vorticity is defined at the regular mesh points by the relations

$$\eta=\delta_z u-\delta_x w=\nabla^2\psi \qquad (2.32)$$

where

$$\nabla^2=\delta_{xx}\psi+\delta_{zz}\psi=\delta_x(\delta_x\psi)+\delta_z(\delta_z\psi).$$

Thus the principal dependent variables η, ψ, and T are not staggered in space or time, but their derivatives are defined at intermediate points.

The finite difference equations of motion, vorticity and temperature will now be displayed in a form adapted from a similar, through somewhat more elaborate, scheme devised by Arakawa (1962):

$$\delta_s\bar{u}^s=\frac{2u-\bar{u}^{2s}}{2}-\overline{(\bar{u}^x-x)\delta_x u}^x-\overline{(\bar{w}^x-z)\delta_z u}^z$$
$$-\delta_x\pi+\nu\nabla^2 u_{\text{lag}} \qquad (2.33)$$

$$\delta_s\bar{w}^s=\frac{2w-\bar{w}^{2s}}{2}-\overline{(\bar{u}^z-x)\delta_x w}^x-\overline{(\bar{w}^z-z)\delta_z w}^z$$
$$-\delta_z\pi+\bar{T}^{xzz}+\nu\nabla^2 w_{\text{lag}} \qquad (2.34)$$

$$\delta_s\bar{\eta}^s=-\frac{\bar{\eta}^{2s}}{2}-\delta_x\overline{[(\bar{u}^z-x)\eta]}^x-\delta_z\overline{[(\bar{w}^x-z)\eta]}^z$$
$$+\delta_x\bar{T}^{xzz}+\nu\nabla^2\eta_{\text{lag}}-\frac{\Delta^2}{2}\delta_{xxzz}\psi \qquad (2.35)$$

$$\delta_s\bar{T}^s=-\delta_x[(\bar{u}^{xz}-x)\bar{T}^x]$$
$$-\delta_z[(\bar{w}^{xz}-z)\bar{T}^z]+\kappa\nabla^2 T_{\text{lag}} \qquad (2.36)$$

where

$$\bar{\varphi}^{2s}=\bar{\varphi}^{ss}+\left(\frac{\Delta s}{2}\right)^2\delta_{ss}\varphi$$

for arbitrary φ. The subscript "lag" on the friction terms indicates that they are evaluated non-centrally at time $s-\Delta s$. This set can be seen to be clearly, but not uniquely, analogous to the corresponding continuous equations. The peculiar term at the end of the vorticity equation (2.35) is a result of the way the coordinate advection (stretching) terms are written. This equation may be directly derived by taking the finite difference curl of (2.33) and (2.34). The particular merit of the above system, as shown in Appendix 1, is that it conserves momentum, energy, temperature, and temperature variance ($T^2/2$) in a manner analogous to that of the continuous system. The conservation of sums of squares of a field is a sufficient condition for computational stability, if by the latter we mean a bounded deviation of the numerical solution from its continuous analog as time approaches infinity. We show in the appendix that, because of the centered time differencing, this scheme does not quite satisfy that condition, although it appears to be completely stable provided that the linear stability criteria are satisfied. The finite difference boundary conditions used were completely analogous to (2.5) and (2.6) at inner and outer boundaries. In addition, auxiliary computational boundary conditions required in the solution of (2.36) were chosen to preserve the integral properties, as outlined by Smagorinsky (1958).

The method of solution consisted of centered time extrapolation of (2.35) and (2.36) (uncentered for the first time step) and exact (within round-off error) solution of the Poisson equation (2.32) by the Ogura-Charney (1962) method. The Courant-Friedrichs-Lewy requirements for maintenance of computational stability are, approximately, that

$$\Delta s<\frac{\Delta}{|u-x|+|w-z|} \qquad (2.37)$$

$$\Delta s<\frac{\Delta^2}{8\nu} \qquad (2.38)$$

$$\Delta s<\frac{\Delta^2}{8\kappa} \qquad (2.39)$$

the first of which turns out in practice to depend entirely on the maximum values of the coordinates, i.e., the boundary locations. Thus each of these may be evaluated from the parameters alone.

From (2.36) it may be shown that the spatial integral of temperature, evaluated by the trapezoidal rule, remains constant, except for boundary effects which can be made negligible by choosing the boundary locations

such that the buoyant element remains well inside them. This integral was initially set to unity, i.e.,

$$\sum_{i=1}^{M-1}\left[\sum_{j=1}^{N-1}(T_{ij})+\tfrac{1}{2}(T_{i0}+T_{iN})\right]+\tfrac{1}{2}\sum_{j=1}^{N-1}(T_{0j}+T_{Mj})+\tfrac{1}{4}(T_{00}+T_{0N}+T_{M0}+T_{MN})=1 \quad (2.40)$$

where

$T_{ij}=T(x,z)$ with $x=i\Delta$, $z=j\Delta$, $D=M\Delta$, and $H=N\Delta$.

For given values of the parameters ν and κ, we hypothesize that the above integral stipulation is the necessary and sufficient condition for a unique steady-state solution of the system, and that we may approach arbitrarily close to this solution by continued time integration from an otherwise arbitrary initial state. Alternative hypotheses include the possibilities of no steady-state solution, more than one such, or a solution which is unstable or neutral to finite perturbations and so cannot be approached asymptotically.

3. Steady state balance requirements

In discussion of our results, we will have occasion to refer to the balance requirements for energy, vorticity, and temperature variance, which will now be derived. The kinetic and potential energy equations in the transformed system are obtained from multiplication of (2.23), (2.24) and (2.25) by u, w, and $-z$ respectively, and may be written:

$$\frac{\partial}{\partial s}\left(\frac{u^2+w^2}{2}\right)+\frac{\partial}{\partial x}\left[(u-x)\left(\frac{u^2+w^2}{2}\right)+u\pi\right]+\frac{\partial}{\partial z}\left[(w-z)\left(\frac{u^2+w^2}{2}\right)+w\pi\right]-wT=\nu\nabla^2\left(\frac{u^2+w^2}{2}\right)-\nu[(\nabla u)^2+(\nabla w)^2] \quad (3.1)$$

$$\frac{\partial}{\partial s}(-zT)+\frac{\partial}{\partial x}[(u-x)(-zT)]+\frac{\partial}{\partial z}[(w-z)(-zT)]+wT=-\kappa\nabla\cdot(z\nabla T)+\kappa\frac{\partial T}{\partial z}. \quad (3.2)$$

Similarly the equations of the temperature variance and the impulse (x-weighted vorticity) may be written:

$$\frac{\partial}{\partial s}\left(\frac{T^2}{2}\right)+\frac{\partial}{\partial x}\left[(u-x)\left(\frac{T^2}{2}\right)\right]+\frac{\partial}{\partial z}\left[(w-z)\left(\frac{T^2}{2}\right)\right]-T^2=\kappa\nabla^2\left(\frac{T^2}{2}\right)-\kappa(\nabla T)^2 \quad (3.3)$$

$$\frac{\partial}{\partial s}(x\eta)+\frac{\partial}{\partial x}[(u-x)x\eta]+\frac{\partial}{\partial z}[(w-z)x\eta]-u\eta+\tfrac{3}{2}x\eta+\frac{\partial}{\partial x}(xT)-T=\nu\nabla\cdot(x\nabla\eta)-\nu\frac{\partial\eta}{\partial x}. \quad (3.4)$$

We shall principally utilize the spatially integrated forms of these equations, in particular integrated over the range $0\leq x<\infty$ and $0\leq z<\infty$. Because of the special coordinate transformation terms in the advective fluxes, it is not clear that the integrals of these terms must vanish at infinity. Making this physical assumption, however, we write the integral forms of (3.1)–(3.4) as follows:

$$\frac{\partial E_k}{\partial s}+E_k-\{E_k:E_p\}=-\epsilon_k \quad (3.5)$$

$$\frac{\partial E_p}{\partial s}+E_p+\{E_k:E_p\}=\kappa\int_0^\infty T|_{z=0}dx \quad (3.6)$$

$$\frac{\partial\sigma_T{}^2}{\partial s}-2\sigma_T{}^2=-\epsilon_T \quad (3.7)$$

$$\frac{\partial I}{\partial s}+\tfrac{3}{2}I-B=-\nu\int_0^\infty x\frac{\partial\eta}{\partial z}\bigg|_{z=0}dx-\int_0^\infty\frac{u^2}{2}\bigg|_{z=0}dx. \quad (3.8)$$

Where the symbols are defined as follows:

$$E_k=\int_0^\infty\int_0^\infty\left(\frac{u^2+w^2}{2}\right)dxdz,\quad E_p=-\int_0^\infty\int_0^\infty zTdxdz,\quad \sigma_T{}^2=\int_0^\infty\int_0^\infty\frac{T^2}{2}dxdz,\quad I=\int_0^\infty\int_0^\infty x\eta dxdz,$$
$$\{E_k:E_p\}=\int_0^\infty\int_0^\infty\bar{w}Tdxdz,\quad \epsilon_k=\nu\int_0^\infty\int_0^\infty\eta^2dxdz,\quad \epsilon_T=\kappa\int_0^\infty\int_0^\infty(\nabla T)^2dxdz,\quad B=\int_0^\infty\int_0^\infty Tdxdz=1. \quad (3.9)$$

The circulation integral will also be of interest. This is obtained by integrating the transformed vorticity equation (2.25) from $x=0$ to ∞:

$$\frac{\partial C}{\partial s}+\frac{C}{2}-\int_0^\infty T\Big|_{x=0}dx=-\nu\left[\int_0^\infty \frac{\partial \eta}{\partial x}\Big|_{x=0}dz+\int_0^\infty \frac{\partial \eta}{\partial z}\Big|_{z=0}dx\right] \tag{3.10}$$

where

$$C=\int_0^\infty\int_0^\infty \eta dxdz.$$

In many cases the lower boundary terms in the above relations are small and may be ignored. Making this assumption, and considering the steady state conditions, for which $\partial/\partial s=0$, we write the balance conditions for energy, temperature variance, impulse, and circulation:

$$E_k=\{E_k: E_p\}-\epsilon_k=-E_p-\epsilon_k \tag{3.11a}$$

$$2\sigma_T{}^2=\epsilon_T \tag{3.11b}$$

$$I=\tfrac{2}{3} \tag{3.11c}$$

$$C=\int_0^\infty\left(T-\nu\frac{\partial \eta}{\partial x}\right)\Big|_{x=0}dz. \tag{3.11d}$$

4. Results of computations

All integrations were performed on a 32×32 grid, including boundaries, with the grid separation equal to either 0.05 or 0.1 non-dimensional units. Calculations were carried out for several values of ν and κ in the range 0.01–0.10, the results of which seemed to include most of the area of physical interest. In all cases a steady solution was approached, but the characteristics of both the transient and final solutions varied considerably from case to case. The initial conditions were generally taken to be either a hemispherical temperature bubble on the lower boundary, as in most previous numerical calculations (Malkus and Witt, Ogura, Lilly) or from the solutions of other cases. Trials indicated that neither the shape-preserving solution nor the time required to approach it were much dependent on the initial condition. The artificiality of the eddy viscosity assumption is perhaps most significant in the transient behavior, since, as shown in Section 2, the coefficients are related only to the nominal space and velocity scales, regardless of the actual momentary intensity or form of the motions. Therefore, we shall postpone discussion of the transients until the end of this section, although their behavior does lead to some clarification of previous numerical results in this field. Figs. 2–5 show the approximately steady state solutions of stream field and temperature for, respectively:

1) $\nu=\kappa=0.01$

2) $\nu=0.04$, $\kappa=0.01$

3) $\nu=0.01$, $\kappa=0.04$

4) $\nu=\kappa=0.04$.

Reconstruction of the real temperature and velocity fields and the length scales could be accomplished by application of (2.22a)–(2.22d).

It should again be pointed out that these assumed eddy coefficients must actually be properties of the complete 3-dimensional fields of motion and temperature. Thus, the above experimental variation of ν and κ does not correspond to an actual variation of physical parameters. Rather, the comparison of results to laboratory data will lead to determining appropriate values of the coefficients. A comparison of the heights and stream function intensities of the various results leads to the rather surprising conclusion that, within the above range of parameters, increased thermal diffusion considerably increases the ascent rate and decreases the angle of expansion. This conclusion is at some variance with the assumptions made by Lilly and Ogura in discussing their numerical results and inertial reference frame models. We may, however, approach an understanding of the effect by consideration of temperature variance, impulse and circulation balance equations (3.11b), (3.11c) and (3.11d). From the first of these, we note that the steady shape regime is impossible to attain without thermal diffusion. This is due to a form of "ultra-violet catastrophe" imposed by the scale-time relationships. From the circulation equation (3.11d) we see that the circulation increases with the temperature along the left boundary (symmetry line) and is diminished by the leaking away of vorticity across it. The circulation itself, however, tends to remove buoyant fluid from the center and replace it with ambient entrained fluid, by a process of continually turning the parcel "inside out." In our non-inertial reference frame the circulation will then decay because of the effect of the second term in (3.10). If this process is not countered by diffusion the temperature will soon be entirely concentrated near the vortex centers. Since the impulse, the x-moment of vorticity, is determined mainly by the total buoyancy, the ratio of impulse to circulation (a horizontal scale length) will increase and the entire element will separate in the center and become a buoyant vortex pair. It is apparently possible to obtain such results physically by imposing

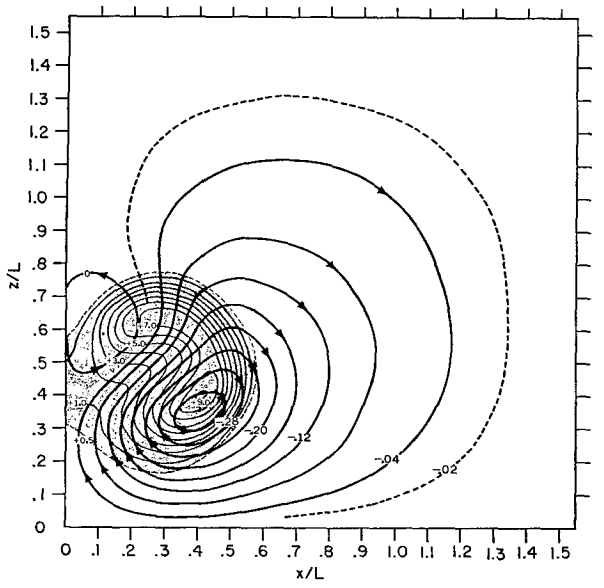

FIG. 2. Dimensionless stream and temperature fields for the shape-preserving solution, case 1, $\nu=\kappa=0.01$. Dimensional scales for length, temperature and stream function are, respectively, $\left(\frac{9}{4}g\alpha Q t^2\right)^{\frac{1}{4}}$, $Q\Big/\left(\frac{9}{4}g\alpha Q t^2\right)^{\frac{1}{4}}$, and $\left(\frac{2}{3}g^2\alpha^2 Q^2 t\right)^{\frac{1}{4}}$.

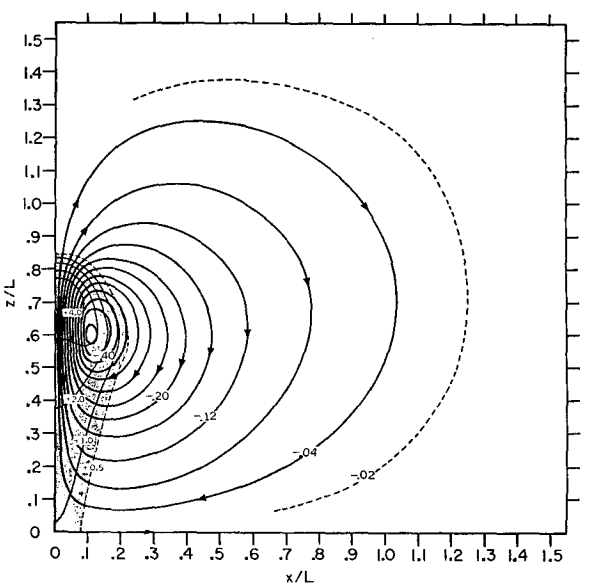

FIG. 3. Case 2, $\nu=0.01$, $\kappa=0.04$. See Fig. 2 caption for details.

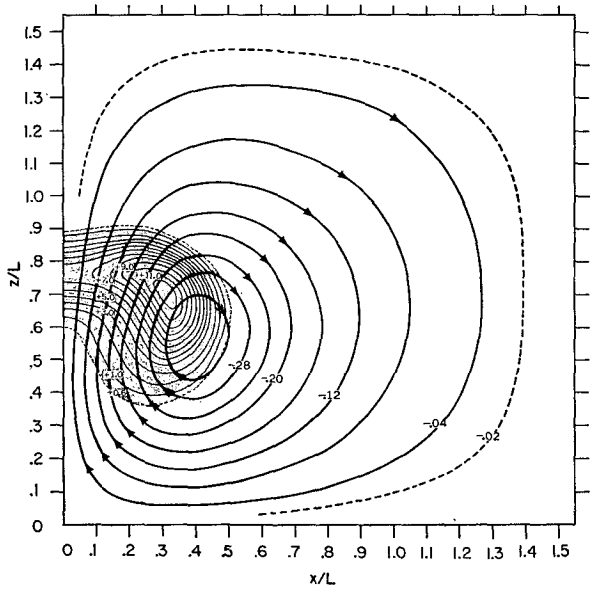

FIG. 4. Case 3, $\nu=0.04$, $\kappa=0.01$. See Fig. 2 caption for details.

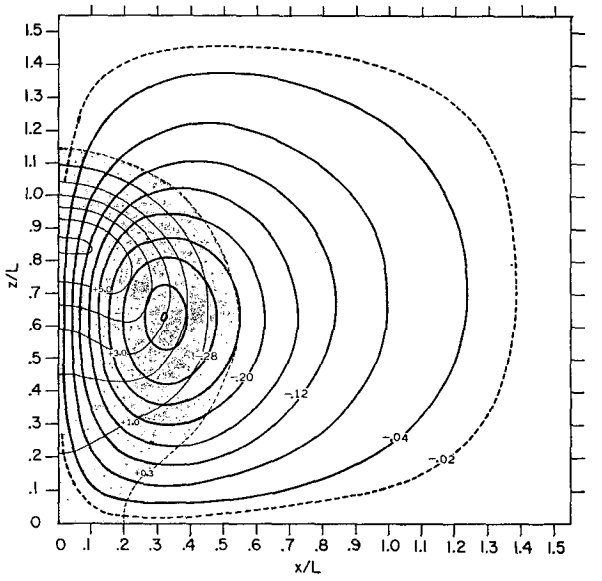

FIG. 5. Case 4, $\nu=0.04$, $\kappa=0.04$. See Fig. 2 caption for details.

an initial momentum push on the parcel (see Turner, 1956, 1960), which causes the vortices to separate before turbulence can be generated sufficient to maintain a mixed central regime. Our results for small ν and κ show an intermediate regime (probably unstable physically) in which the vortices are nearly, but not quite, separated, a narrow saddle-point in the temperature field providing the only connection. The effect of variation of viscosity is apparently less notable, and may perhaps be principally related to the vorticity diffusion term in the circulation equation.

Before exhibiting quantitative comparisons of the numerical results with laboratory measurements it would be desirable to dispose of the uncertainties introduced by the replacement of infinite boundary conditions by the finite closed boundary in our non-inertial

TABLE 1. A comparison of properties of laboratory buoyant elements, observed by Richards, with those measured from the steady state results of our 4 cases. (See text for explanation of symbols.)

Quantity	Laboratory realizations							Numerical cases			
	A	B	C	D	E	Error	Avg.	1	2	3	4
n	2.02	2.20	2.11	2.49	1.86	5	2.14	1.33	1.80	3.58	2.13
c	0.54	0.48	0.53	0.56	0.47	8	0.52	0.65	0.65	0.70	0.52
$C/Z\dot{Z}$	1.14	0.91	1.36	0.65	1.40	12	1.09	1.69	1.93	1.21	1.60
$w_{max}/\dot{Z}$	1.5	1.4	1.8	1.0	1.6	10	1.46	1.12	1.30	1.86	1.49
$\dot{Z}\sqrt{R/B}$	0.69	0.88	0.65	0.64	0.68	8	0.71	0.42	0.48	0.84	0.59
E_K/E_P	0.40	0.33	0.37	0.22	0.58	15	0.38	0.43	0.32	0.54	0.35

reference frame. In Appendix 2, this problem is discussed in some detail. Some approximate, but perhaps sufficiently convincing, calculations described therein lead to the conclusion that the errors introduced are indeed negligible.

Table 1 shows a comparison of properties of laboratory buoyant elements, observed by Richards, together with those measured from the steady state results of 4 cases. The quantities listed are defined as follows:

n—the ratio of Z, the height of the element's front, to R, its half-width at the widest point. For our purposes, the height and width were defined by the isotherm T_b, where $T_b=0.05$ of T_{max}, the maximum temperature. These would be little changed for $0.01<T_b/T_{max}<0.10$.

c—the ratio of the height of the widest part of the element to that of its front.

$C/Z\dot{Z}$—ratio of circulation to height times velocity of the element's front.

$w_{max}/\dot{Z}$—ratio of maximum vertical velocity to front velocity.

$\dot{Z}(R/B)^{\frac{1}{2}}$—inverse square root of the drag coefficient, where B is the total buoyancy (2 in the dimensionless system).

$-E_k/E_p$—ratio of kinetic to released potential energy (measured from the time rates in the laboratory results).

The first two of these statistics relate to the geometrical shape of the element, the next two to its kinematics, and the last two to its dynamic properties. It is evident that the results of case 4 are in good agreement with the average of the laboratory results, although the latter exhibit a great deal of spread. The two greatest discrepancies, the circulation ratio and drag coefficient, could be improved somewhat by defining 0.01 T_{max} as the edge, with little change occurring in the other ratios.[1] As we noted qualitatively before, an increase in the diffusion coefficient increases the rate of ascent and decreases the drag coefficient and entrainment. Increasing the viscosity causes an increase in dissipation (E_k/E_p decreases) and entrainment, a decrease in maximum velocity, and other somewhat less clear-cut effects. Although Scorer (1957) has observed that turbulent mixing is most intense near the front, where the Richardson number is large and negative, the assumption of a spatially constant viscosity and diffusion seems to explain the gross characteristics of the buoyant element. As pointed out earlier, turbulent diffusion serves the important purpose of holding the element together in the center, thus maintaining a high correlation between w and T and preventing a separation of the vortices. Since the center is a region of relatively small thermal gradients, most of the turbulence in this region has flowed or diffused in from more active areas. It is therefore probably relatively isotropic and homogeneous and diffuses temperature and momentum more-or-less equally and inertly.

It may be seen from the temperature equation in the transformed variables (2.26) that the effective advecting flow consists of the wind vector minus the radius

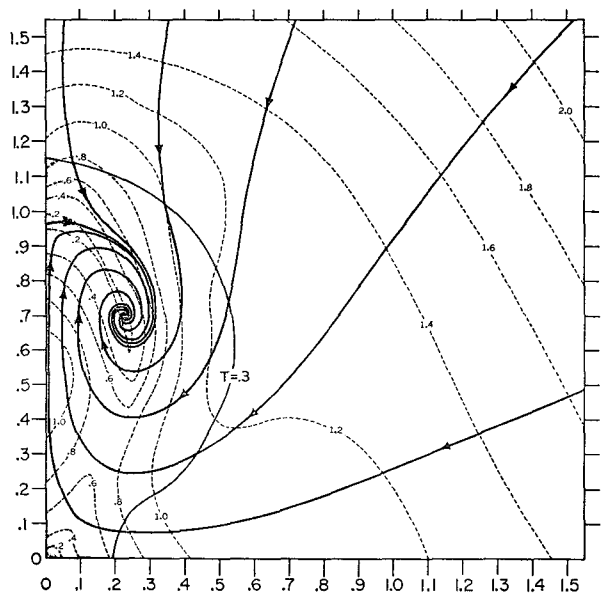

FIG. 6. Trajectories and isotachs relative to the shape-preserving solution of case 4, $\nu=\kappa=0.04$. The dimensional velocity scale is $\frac{2}{3}\left(\frac{g\alpha Q}{t}\right)^{\frac{1}{3}}$. See Fig. 2 for other details.

[1] After a final copy of Richards' results became available, it was noted that most of his results, including those in Table 1, were obtained from elements released internally, i.e., well away from a boundary. A similar numerical computation has been performed, but the results differ only slightly from the above.

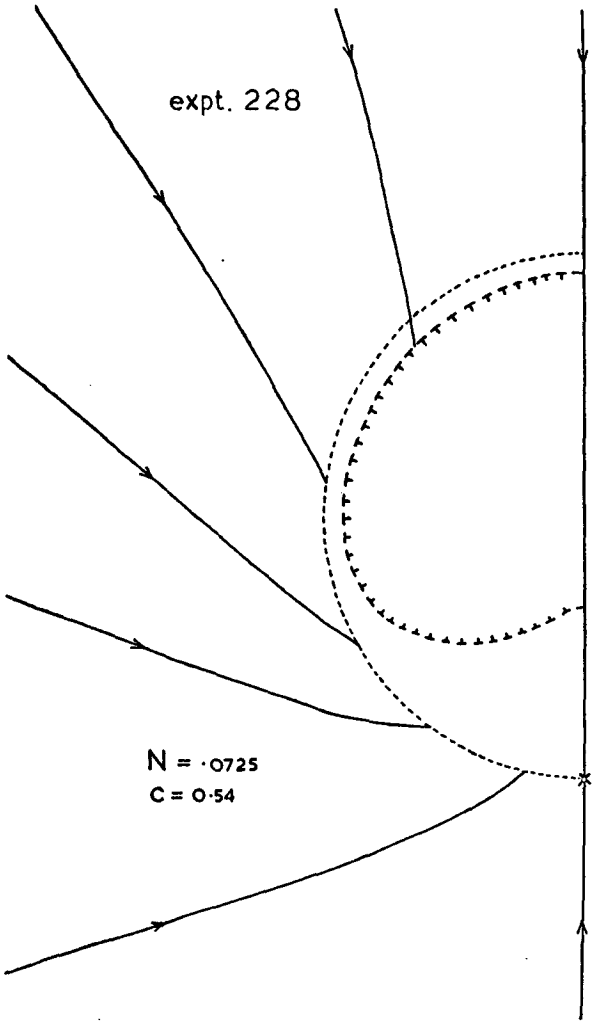

FIG. 7. Trajectories relative to the experimentally observed shape-preserving elements for strong circulation cases (figure from J. M. Richards).

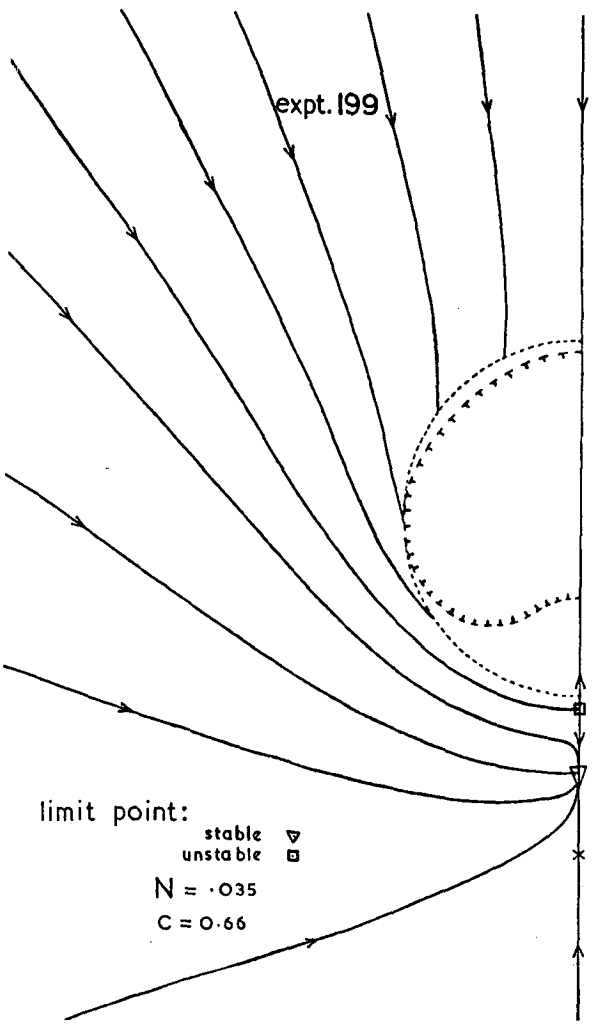

FIG. 8. Trajectories relative to the experimentally observed shape-preserving elements for weak circulation cases (figure from J. M. Richards).

vector. The resulting flow will define streamlines or trajectories (in the steady state) relative to the expanding elements. The field of relative streamlines and isotachs for case 4 is depicted in Fig. 6, where the shaded area is circumscribed by the $0.05T_{\max}$ isotherm. We note that all the flow lines converge to a point near but not precisely at the vortex center. Richards found similar patterns in many of his experimental vortices, including the five cases summarized in Table 1. For others, in which the vortex circulation was weaker, a second convergent point was found behind the element, with a hyperbolic point and line of difluence separating trajectories that flowed into the element from those remaining outside it. Figs. 7 and 8, taken from Richards' thesis (1961), show these characteristic flow patterns. Further details are given in the thesis.

A few miscellaneous interesting statistics of the case 4 results may be mentioned. The ratio of horizontal to vertical kinetic energy is 0.5. The correlation between vertical motion and temperature is 0.67. The eddy Reynolds number, based on the maximum velocity and the average distance from the point of maximum temperature to the isotherm $T=e^{-0.5}T_{\max}$ is about 10. This may be compared with the values given by Townsend (1956) for line and axially symmetric wakes of 12.5 and 14.1, respectively, and 27 and 32 for line and axially symmetric jets. The eddy Rayleigh number is simply $2/\nu\kappa$, or 1250. In this regard, a solution analogous to that of Morton's axisymmetric weak thermal vortex has been derived (not presented here) from equations (2.26), (2.27) for small Rayleigh number (order 10), Prandtl number unity, and fully infinite boundary conditions (no lower boundary). The only statistic which can be properly compared to our results is the energy ratio $-E_k/E_p$, which turns out to be exactly $\frac{1}{3}$, rather surprisingly (and perhaps coincidentally) close to the value

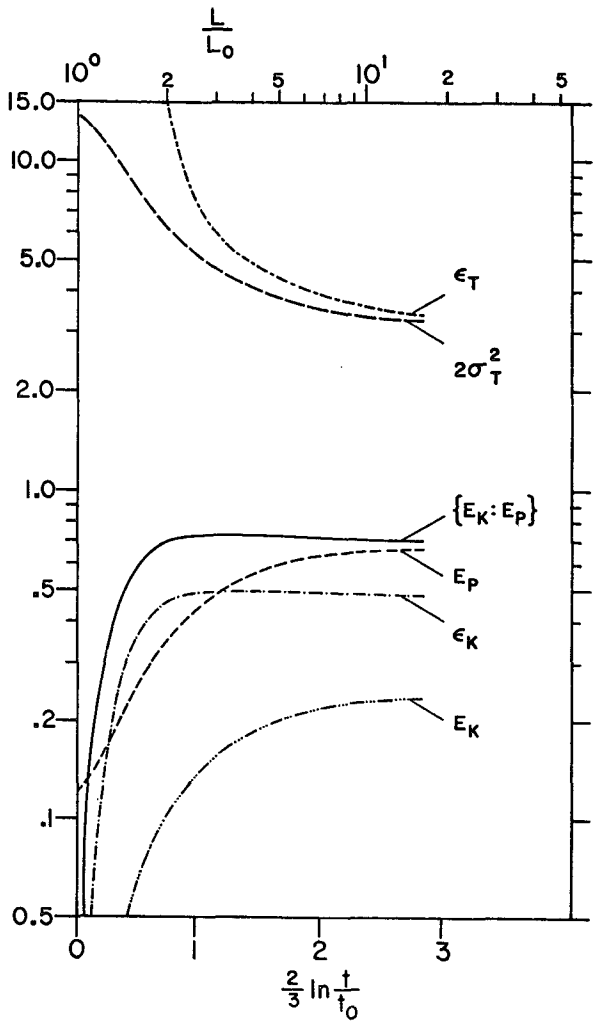

FIG. 9. Integral quantities as functions of the dimensionless time and length scales, case 4, $\nu=\kappa=0.04$. E_K is kinetic energy, E_P potential energy, $\{E_K:E_P\}$ the potential to kinetic energy transformation, ϵ_K kinetic energy dissipation, ϵ_T temperature variance dissipation, σ_T^2 temperature variance, all in dimensionless measures.

for case 4. The effective area of moving fluid may be defined analogously to the virtual mass of a moving cylinder, by the ratio of total kinetic energy to the average ascent velocity of the element. This area is approximately equal to unity, or about 2.2 times the area in which $T>0.05T_{\max}$. This corresponds rather closely to the value 2.0 for a moving cylinder in an ideal fluid, as was first pointed out to me by C. Rooth (personal communication).

We now turn to consideration of the transient behavior of our solutions. Case 4 was started from initial conditions similar to those of Malkus-Witt's and Lilly's previous numerical experiments, that is, a semicircular thermal disturbance at the bottom of a motionless isothermal fluid. The behavior during the initial acceleration stage was similar to the earlier results, except for the concentration effects of the coordinate transformation terms. Fig. 9 shows the integrated kinetic and potential energies, energy transformation, twice the thermal variance, and dissipations for case 4 on a logarithmic scale, plotted against the non-dimensional time coordinates, where we recall that

$$s=\tfrac{2}{3}\ln\frac{t}{t_0}=\ln\frac{L}{L_0}.$$

All quantities approach their asymptotic values quite uniformly except the energy transformation term $\{E_k:E_p\}$, which overshoots slightly in the intermediate stages. From equations (3.11a, b) we see that in the steady state $E_p=-\{E_k:E_p\}$ and $2\sigma_T^2=\epsilon_T$, to within limits imposed by the boundary conditions. The curves in Fig. 9 show that these relations are closely approached in a period of time corresponding to a 12-fold increase in the length scale. Evaluation of the time derivative terms in the complete equations (3.5)–(3.7) indicates that the deviation from the steady state is of the same order as the boundary error.

Fig. 10 shows the same curves for case 1. The initial conditions for this case were taken from the steady state solution of case 4. The striking difference in transient behavior is caused by a largely nonlinear oscillation in the height and shape of the element, which also occurs if the initial conditions are the same as for case 4. This oscillation is further illustrated by Figs. 11 and 12, which portray the solutions at $s=0.4$ and $s=4.8$, near the peak and valley, respectively, of the primary oscillation of E_p. At the peak the element is tall and thin with a strong concentrated central updraft. Then, as the temperature maximum begins to split away from the center, the correlation between w and T diminishes rapidly and the kinetic energy, negative potential energy, circulation, and height drop because of the coordinate transformation effects, but the width continues to increase because the impulse relation depends principally only on net buoyancy. As the element approaches the lower boundary, however, the symmetry condition causes a separation of the vortex center and the center of vorticity—the latter being closer to the boundary. Thus the vortex advects itself inward and, upon approaching the origin, upward. The temperature maximum partially returns toward the z-axis and a small reverse circulation is formed above the element as steady state is approached. It is probable that this return would not occur in a physical experiment since, once a separated vortex pair is established, rotational stability may cause turbulent diffusion to virtually disappear. The vortices would then shrink in the transformation space as rapidly as they approached the boundary.

In the attempted numerical simulations of buoyant

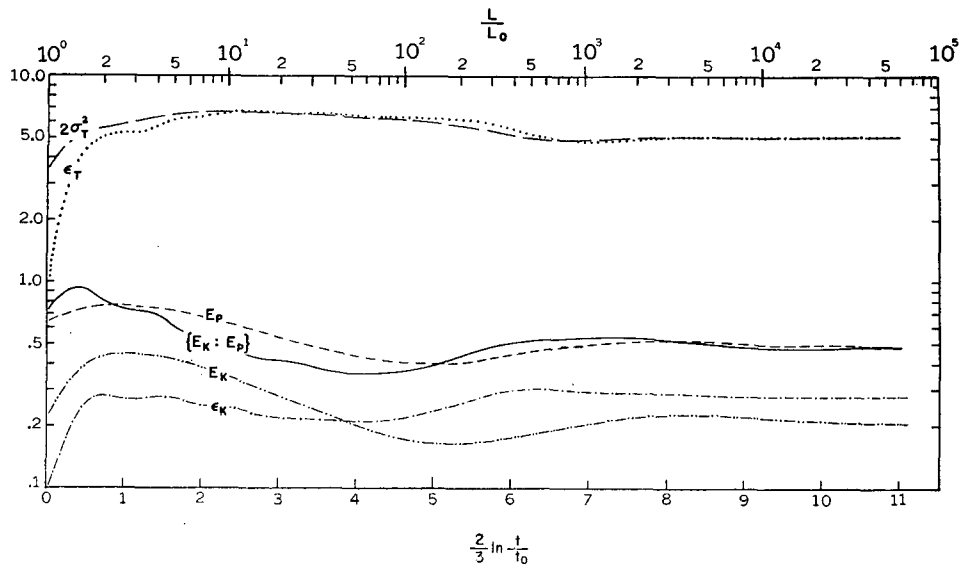

FIG. 10. Integral quantities, Case 1, $\nu = \kappa = 0.01$, see Fig. 9 caption for details.

elements in an inertial reference frame both Lilly and Ogura noted that, by comparison with laboratory measurements, the computer-simulated elements were generally too narrow and intense. This was probably correctly attributed to insufficient viscous damping, since in both models the effective viscosity and diffusion (variable in space and time) tended to decrease in the later stages of development of the element. We note from our steady state results that decreasing the viscosity and diffusion together results in a lower, squatter element with smaller velocities. The transient behavior, however, is rather consistent with the inertial model results. At the peak of the first oscillation in case 1, the values of n, c, E_k/E_p, and $w_{\max}/\dot{Z}$ were, respectively, 2.40, 0.61, 0.60, and 2.40, corresponding roughly to those of Lilly's inertial frame model. Since the available size of the computational grid in the inertial model experiments was such that an element hit the top of the "tank" before having expanded more than a few times its initial diameter, it may be assumed that the transient phase was rather far from completion. The apparent near-attainment of the similarity region in Ogura's results may only have been the attainment of the first transient peak, or it may have signified a different and essentially computational similarity regime, related to the continually decreasing effective viscosity. A recent note by Richards (1963b) calls attention to the rather wide range of experimental modes obtained by Scorer, Woodward and himself in individual experimental realizations under presumably identical initial conditions. This apparent non-reproducibility is evident in the results quoted in Table 1, for example. Whether there really are many possible shape-preserving regimes or only slow large-amplitude variations about a single mode is undetermined. It is very doubtful whether two-dimensional calculations of the sort done previously and in this investigation can shed much light on the subject.

5. Conclusions and outlook

We have shown that the shape-preserving buoyant thermal element can be simulated by the numerical solution of a Boussinesq system transformed through time dependent length and temperature scales into a form in which the shape-preserving solution becomes steady state. Upon introduction of spatially constant eddy-viscosity and diffusion coefficients steady state solutions are approached as the asymptotic limits of time dependent solutions, for a range of values of the coefficients. For ν and κ both equal to 0.04 of the product of the length scale and its time derivative the steady state solution shows good quantitative agreement with the buoyant elements studied by Richards. The solutions are of somewhat the same general class as the one-dimensional approximations to steady state wake and jet flows (see, e.g., Townsend) and, like them, undoubtedly lack accuracy in detail near the edges. The complications of the phenomena which make it difficult to solve for the steady state analytically, two dimensions and two dynamically coupled dependent variables, also add interest to the approximations obtained.

The role of temperature diffusion in the central and upper portions is seen to be critical to the formation and maintenance of the convective element. If diffusion is lessened appreciably, there is a distinct tendency for the element to separate into two buoyant vortex pairs with consequent complete alteration of its energetics. Eddy viscosity apparently exerts less critical effects on the dynamics. Boundary conditions, both physical and computational, have relatively small influence on the

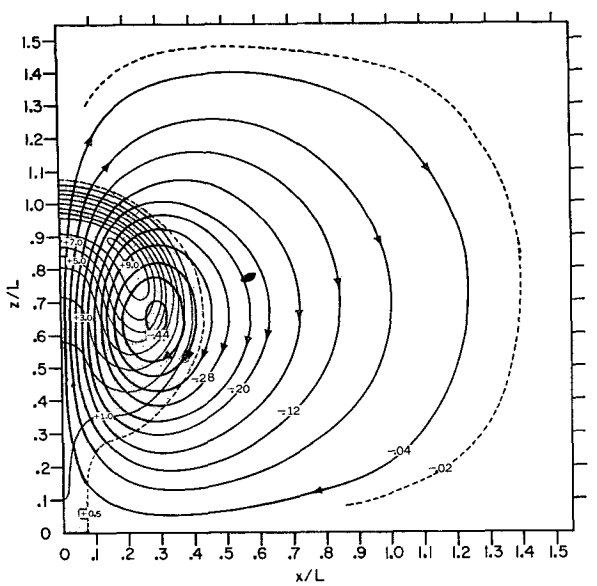

FIG. 11. Stream and temperature fields for case 1, $\nu=\kappa=0.01$ at the time of maximum energy, $s=0.4$.

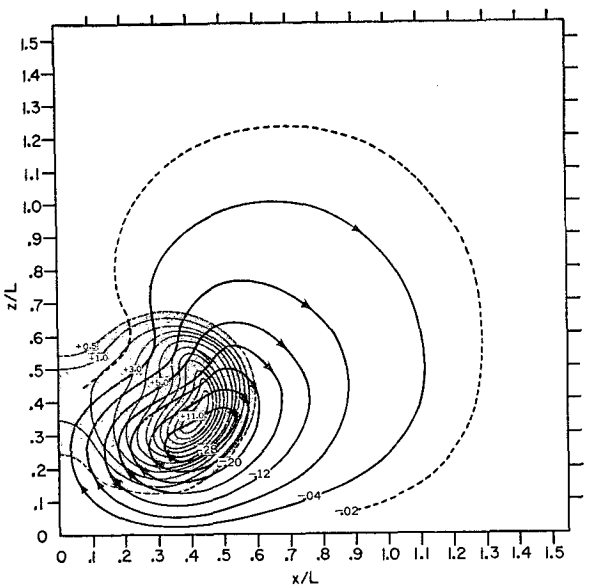

FIG. 12. Stream and temperature fields for case 1, $\nu=\kappa=0.01$ at the time of minimum energy, $s=4.8$.

shape-preserving element, since values of buoyancy and vorticity are negligibly small in the vicinity of the boundaries.

It is impossible to list the many aspects of thermal convection which might be investigated by numerical methods such as were used in this study. Several able investigators are presently actively engaged in similar work relating moist and dry motions of various scales, laminar and turbulent, and in some cases involving important boundary conditions. The most obvious immediate application of the particular methods described here would be in the extension to the axially symmetric case. Work in this area is presently in progress.

It must be noted, however, that the rather empirical methods of dealing with turbulent diffusion such as were applied in this paper and previous work (Lilly, 1962) will probably continue to be the rule so long as two-dimensional space is used in describing inherently three-dimensional motions. Computer technology is advancing to the point where correct representations of three-dimensional turbulent motions may soon be feasible, at least in a highly simplified physical context. Whether such studies can add to our present poverty of understanding of turbulent transfers is yet to be seen.

Acknowledgments. I wish to gratefully acknowledge the extremely able assistance of Mr. G. Daniel Hembree, who performed most of the computer programming, supervised the preparation of display material, and offered valuable suggestions and criticisms on the work. Thanks are due also to Drs. K. Bryan, S. Manabe and J. Smagorinsky for their suggestions and criticisms. The computations were accomplished on the Numerical Weather Prediction Unit IBM 7090 and on the General Circulation Research Laboratory IBM 7030 (STRETCH).

APPENDIX 1

Conservation and Stability Properties of the Finite Difference Scheme

We will here show that energy and variance conservation equations analogous to (3.5)–(3.11) may be derived from the finite difference equations (2.30)–(2.33) together with boundary conditions analogus to those of the continuous system. In order to derive the conservation equations with reasonable economy of space, it is desirable to introduce a set of finite difference and sum identities and definitions, some of which are related to differential calculus rules. A sufficient set for the present purposes is the following, where φ and ψ are arbitrary functions of the discrete variable $x_i=i\Delta$.

$$\begin{aligned} &\text{(a)}\quad \varphi\delta_x\psi=\delta_x(\bar{\varphi}^x\psi)-\delta_x\varphi\cdot\psi^x \\ &\text{(b)}\quad \bar{\varphi}^x\delta_x\varphi=\delta_x(\varphi^2)/2. \end{aligned} \tag{A1}$$

The above identities, and others relating products and quotients of averages and differences, may be proven from definitions (2.26), recognizing that the bar and delta operators are linear, commutative, and distributive, so that, e.g., $\delta_x\bar{\varphi}^{xy}=\overline{(\delta_x\varphi)}^{xy}=\overline{\delta_x\bar{\varphi}^x}^y$, and $\bar{\varphi}^x+\bar{\psi}^x=\overline{(\varphi+\psi)}^x$, etc.

We now exhibit a detailed partial derivation of the finite difference temperature variance equation, to illustrate the method and power of the above notation and identities. Since the core of the problem lies in the advection terms, we start with a simplified version of

(2.33), including only those terms, i.e.,

$$\delta_s\bar{T}^s=-\delta_x(\bar{u}^{xz}\bar{T}^x)-\delta_z(\bar{w}^{xz}\bar{T}^z)-\frac{T}{2}(\delta_x\bar{u}^{xz}+\delta_z\bar{w}^{xz}) \quad \text{(A2)}$$

where the terms of the continuity equation have been added to the right side, averaged over x and z and multiplied by $T/2$. Upon multiplication of (A2) by T and application of rule (a) we obtain:

$$\delta_s[(\bar{T}^s)^2]-\bar{T}^s\delta_sT=-\delta_x[\bar{u}^{xz}(\bar{T}^x)^2]-\delta_z[\bar{w}^{xz}(\bar{T}^z)^2]$$
$$-\overline{\bar{u}^{xz}\bar{T}^x\delta_xT}^x-\overline{\bar{w}^{xz}\bar{T}^z\delta_zT}^z-\tfrac{1}{2}\delta_x(\overline{\bar{u}^{xz}T^2}^x)-\tfrac{1}{2}\delta_z(\overline{\bar{w}^{xz}T^2}^z)+\tfrac{1}{2}\overline{\bar{u}^{xz}\delta_x(T^2)}^x+\tfrac{1}{2}\overline{\bar{w}^{xz}\delta_z(T^2)}^z. \quad \text{(A3)}$$

We now apply rule (b) to the second term on the left and the third and fourth on the right and after a number of cancellations arrive at a flux divergence form of the temperature variance equation, that is

$$\delta_s\left[(\bar{T}^s)^2-\left(\overline{\frac{T^2}{2}}^s\right)\right]=-\delta_x\left\{\bar{u}^{xz}\left[(\bar{T}^x)^2-\left(\overline{\frac{T^2}{2}}^x\right)\right]\right\}-\delta_z\left\{\bar{w}^{xz}\left[(\bar{T}^z)^2-\left(\overline{\frac{T^2}{2}}^z\right)\right]\right\}. \quad \text{(A4)}$$

The combination of product averages appearing in all three terms of (A4) may be written in various ways in the present notation, but it is simply the product of adjacent mesh point values. Defining this combination by the tilde operator we write, for example:

$$\widetilde{TT}^x=2(\bar{T}^x)^2-\overline{T^2}^x=T\left(x+\frac{\Delta}{2},z,s\right)\cdot T\left(x-\frac{\Delta}{2},z,s\right).$$

The complete temperature variance equation, obtained from (2.33) by similar manipulations to those used in deriving (A4), can now be written as follows:

$$\tfrac{1}{2}\delta_s(\widetilde{\widetilde{TT}}^s)=-\delta_x\left[(\bar{u}^{xz}-x)\frac{\widetilde{\widetilde{TT}}^x}{2}\right]-\delta_z\left[(\bar{w}^{xz}-z)\frac{\widetilde{\widetilde{TT}}^z}{2}\right]$$
$$+T^2+\kappa[\delta_x(\bar{T}^x\delta_xT_{\text{lag}})+\delta_z(\bar{T}^z\delta_zT_{\text{lag}})-\overline{\delta_xT\cdot\delta_xT_{\text{lag}}}^x-\overline{\delta_zT\cdot\delta_zT_{\text{lag}}}^z]. \quad \text{(A5)}$$

This equation is analogous to the continuous form (3.3). In order to form the integrated version, analogous to (3.7), one uses trapezoidal rule integration. The terms inside δ_x and δ_z vanish in the summation except near the boundaries. At the left hand boundary ($x=0$) these residual terms are:

$$\overline{\bar{u}^{xz}\left[\frac{\widetilde{\widetilde{TT}}^x}{2}\right]}^x-\kappa\overline{\delta_x(\bar{T}^x\delta_xT_{\text{lag}})}^x.$$

The symmetry boundary conditions $u=\delta_{xx}u=0$, $\delta_x\bar{T}^x=0$ are sufficient to eliminate these terms, and similarly for the lower boundary. At the outer boundaries the requirements are slightly more complex but essentially analogous to those of the continuous system. The kinetic and potential energy equation are derivable in finite difference form in a tedious but straightforward manner. These may be written, respectively, as follows:

$$\tfrac{1}{2}\delta_s(\overline{\widetilde{uu}^s}^z+\overline{\widetilde{ww}^s}^x)+\delta_x\left[\overline{(\bar{u}^x-x)\frac{\widetilde{uu}^x}{2}}^z+\overline{(\bar{u}^z-x)\frac{\widetilde{ww}^x}{2}}^x+\overline{\bar{u}^x\pi}^z\right]$$
$$+\delta_z\left[\overline{(\bar{w}^x-z)\frac{\widetilde{uu}^z}{2}}^z+\overline{(\bar{w}^z-z)\frac{\widetilde{ww}^z}{2}}^x+\overline{\bar{w}^z\pi}^x\right]-\overline{w\bar{T}^{xzz}}^x+\tfrac{1}{2}(\overline{\widetilde{uu}^{sz}}^s+\overline{\widetilde{ww}^{sz}}^s)$$
$$=\nu[\delta_x(\overline{\bar{u}^x\delta_xu_{\text{lag}}}^z+\overline{\bar{w}^x\delta_xw_{\text{lag}}}^x)+\delta_z(\overline{\bar{u}^z\delta_zu_{\text{lag}}}^z+\overline{\bar{w}^z\delta_zw_{\text{lag}}}^x)-\overline{\delta_xu\cdot\delta_xu_{\text{lag}}}^{xz}-\overline{\delta_zu\cdot\delta_zu_{\text{lag}}}^{zz}$$
$$-\overline{\delta_xw\cdot\delta_xw_{\text{lag}}}^{xz}-\overline{\delta_zw\cdot\delta_zw_{\text{lag}}}^{xz}] \quad \text{(A6)}$$

$$\delta_s(-z\bar{T}^s)+\delta_x[(\bar{u}^{xz}-x)z\bar{T}^x]+\delta_z[(\bar{w}^{xz}-z)z\bar{T}^z]-\overline{z\bar{T}^z}+\overline{\bar{w}^{xz}\bar{T}^z}=-\kappa[\delta_x(z\delta_xT_{\text{lag}})+\delta_z(z\delta_zT_{\text{lag}})-\delta_z\bar{T}^z{}_{\text{lag}}]. \quad \text{(A7)}$$

The energy transformation term, which appears to differ between (A6) and (A7), becomes identical in the integral since one may be transformed into the other with the introduction of additional difference terms which integrate out upon application of boundary conditions.

We see that, aside from dissipation and the special terms arising from our non-inertial coordinate system, there are quantities analogous to the total energy and temperature variance which are invariant with time in the spatial integral. Those quantities involve cross products at adjacent time steps, defined by the tilde operator, and their invariance properties are pertinent to the continuous analogue only if the solution behaves smoothly in time. If, on the other hand, the dependent variable solutions at odd and even time steps become decoupled and diverge, the two separate solutions of the difference equations will lose relevance to the differential equation solutions and ultimately some form of catastrophic computational instability will ensue. The possibility of splitting of solutions is a well known property of the "leapfrog" method of time differencing and is known to occur in certain types of linear computational instability, i.e., those associated with non-fulfillment of the Courant-Friedrichs-Lewy criterion. It has proven difficult to investigate splitting associated with non-linear terms but a recent study indicates that splitting occurs, although rather slowly, in a simple set of equations without small scale forcing terms, such as is used in the calculations presented here.

APPENDIX 2

The Finite Approximation to Infinite Boundary Conditions

It seems impossible to dispose of the boundary uncertainties in a complete and rigorous manner, principally because of the non-linear interactions of the stream and temperature fields. We shall therefore proceed heuristically. We first note that in the infinite system, since u, w, and T must all tend toward zero as $x, z \to \infty$, the fluxes of heat must also vanish. Therefore, from (2.23), we have

$$\kappa\frac{\partial T}{\partial x}+xT\to 0 \quad \text{as} \quad x\to\infty \quad \text{(B1)}$$

$$\kappa\frac{\partial T}{\partial z}+zT\to 0 \quad \text{as} \quad z\to\infty, \quad \text{(B2)}$$

and the solution for T must become $\propto e^{-(x^2+z^2)/2\kappa}$ for large x and z. Perhaps the most suitable finite boundary condition for the temperature equation, then, would consist of (B1) and (B2) applied at $x=D$, $z=H$, since these conditions would eliminate boundary fluxes. In fact, trials indicate that it makes little difference whether the boundary conditions applied are the above, the vanishing of the normal derivative, or the vanishing of T itself. In all cases, there is a slight tendency toward boundary-induced instability in the difference equations during the developing phase of the flow, which ultimately damps out as steady state is approached.

The vorticity equation is of the fourth order in the spatial stream derivatives and therefore requires two conditions on each finite boundary. By analogy with the thermal equation, we may specify η, its normal derivative, or its flux to vanish at the outer boundary, and provided that the boundary temperature disturbance is zero or small the effect of any of these on total circulation will be slight. For the other condition, however, we are strongly impelled, because of the method of solving the Poisson equation, to set $\psi=0$ on all boundaries. This is probably the most significant of the finite boundary constraints. To evaluate the error caused thereby we need to solve a rather classical and, in principle, simple problem in fluid dynamics: to find the velocity fields given a known distribution of vorticity (vanishing outside certain bounds) with velocity vanishing at infinity. In a continuum, this solution may be written formally

$$\psi(x,z)=\int_{-\infty}^{\infty}\int_{-\infty}^{\infty}\eta(\xi,\zeta)\cdot G(x,z,\xi,\zeta)d\xi d\zeta \quad \text{(B3)}$$

where

$$G=2\pi\ln[(x-\xi)^2+(z-\zeta)^2]^{\frac{1}{2}}$$

is the Green's function of dummy variables ξ, ζ for an infinite plane. Since our inner boundary conditions imply an antisymmetric vorticity and stream field across x, $z=0$, equation (B3) may be rewritten

$$\psi(x,z)=\int_{0}^{\infty}\int_{0}^{\infty}\eta(\xi,\zeta)\cdot G^*(x,z,\xi,\zeta)d\xi d\zeta \quad \text{(B4)}$$

where

$$G^*=2\pi\ln\left[\frac{(x-\xi)^2+(z-\zeta)^2}{(x+\xi)^2+(z-\zeta)^2}\cdot\frac{(x-\xi)^2+(z+\zeta)^2}{(x+\xi)^2+(z+\zeta)^2}\right]^{\frac{1}{2}}.$$

McCrea and Whipple (1940) have derived the finite difference Green's function for infinite boundaries and showed that it differs from G by a function of order $\Delta^2/[(x-\xi)^2+(z-\zeta)^2]$. We shall neglect this higher order term and further assume that outside of the region $x=D$, $z=H$ (the finite difference boundaries) (B4) may

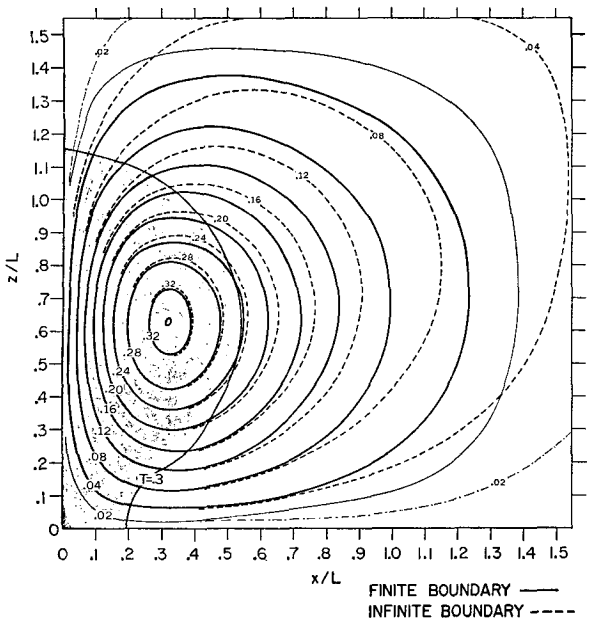

FIG. 13. Dimensionless stream field for the shape-preserving solution $\nu=\kappa=0.04$ (solid lines), with approximate correction for finite boundary effects (dashed lines). Shaded area indicates the nominal extent of the thermally active region. See Fig. 2 caption for other details.

be approximated by

$$\psi(x,z)=G^*(x,z,x',z')\cdot\int_0^H\int_0^D \eta(x,z)dxdz \qquad \text{(B5)}$$

where

$$x'=\frac{\int_0^H\int_0^D x\eta dxdz}{\int_0^H\int_0^D \eta dxdz};\quad z'=\frac{\int_0^H\int_0^D z\eta dxdz}{\int_0^H\int_0^D \eta dxdz}. \qquad \text{(B6)}$$

Equation (B5) holds precisely (in the continuum) for a point vortex of strength $\int_0^H\int_0^D \eta dxdz/2\pi$, or if vorticity is distributed with circular symmetry about x', z'. For our results it is only a first approximation, but a fairly good one, provided that most of the vorticity is distant from the outer boundaries. We have computed the stream field at the boundary $x=D$, $z=H$ from our known vorticity distribution using (B5) and (B6) and applied it as a boundary condition for an exact solution of the finite difference Poisson equation inside. The resulting stream field for case 4 is depicted in the dashed lines of Fig. 13, together with the stream field (solid lines) computed from the usual finite boundary conditions. The net change of velocity inside the thermally active region (shaded area) is slight and suggests that an infinite boundary would promote a slightly higher and narrower element with slightly larger energy, all corrections of the order of 1 per cent.

REFERENCES

Arakawa, A., 1962: The life cycle of large-scale disturbances. Paper delivered at the Fourth Numerical Prediction Conference, 31 Jan.–3 Feb. 1962, Los Angeles, Calif.

Batchelor, G. K., 1954: Heat convection and buoyancy effect in fluids. *Quart. J. R. meteor. Soc.*, **80**, 339–358.

Kuo, H. L., 1961: Solution of the non-linear equations of cellular convection and heat transport. *J. fluid Mech.*, **10**, 611–634.

Levine, J., 1959: Spherical vortex theory of bubble-like motion in cumulus clouds. *J. Meteor.*, **16**, 653–662.

Lilly, D. K., 1962: On the numerical simulation of buoyant convection. *Tellus*, **14**, 148–172.

Malkus, J. S., and G. Witt, 1959: The evolution of a convective element: a numerical calculation. *The atmosphere and the the sea in motion*, New York, Rockefeller Institute Press, 509 pp.

McCrea, W. H., and F. J. W. Whipple, 1940: Random paths in two and three dimensions. *Proc. Roy. Soc.*, Edinburgh, **60**, 281–298.

Morton, B. R., 1960: Weak thermal vortex rings. *J. fluid Mech.*, **9**, 107–118.

—, G. I. Taylor and J. S. Turner, 1956: Turbulent gravitational convection from maintained and instantaneous sources, *Proc. Roy. Soc.*, Ser. A, **234**, 1–23.

Ogura, Y., 1962: Convection of isolated masses of buoyant fluid: A numerical calculation. *J. atmos. Sci.*, **19**, 492–502.

——, and J. G. Charney, 1962: A numerical model of thermal convection in the atmosphere. *Proceedings of the International Symp. on Numerical Weather Prediction*, Tokyo, Nov. 7–13, 1960, Meteor. Soc. of Japan, 656 pp.

Richards, J. M., 1961: Ph.D. Thesis, University of London.

——, 1963a: Experiments on the motion of isolated cylindrical thermals through unstratified surroundings. *Internat. J. Air. Water Poll.*, **17**, 17–34.

——, 1963b: Comparisons between calculated thermal motions and experiments. *J. atmos. Sci.*, **20**, 241–242.

Saunders, P. M., 1961: An observational study of cumulus. *J. Meteor.*, **18**, 451–467.

Scorer, R. S., 1957: Experiments on convection of isolated masses of buoyant fluid. *J. fluid Mech.*, **2**, 583–594.

——, 1959: The behavior of chimney plumes. *Internat. J. air Poll.*, **1**, 198–220.

——, and F. H. Ludlam, 1953: Bubble theory of penetrative convection. *Quart. J. R. meteor. Soc.*, **79**, 94–103.

Shuman, F. G., 1962: Numerical experiments with the primitive equations. *Proceedings of the International Symp. on Numerical Weather Prediction.* Tokyo, Nov. 7–13, 1960, Meteor. Soc. of Japan, 656 pp.

Smagorinsky, J., 1958: On the numerical integration of the primitive equations of motion for baroclinic flow in a closed region. *Mon. Wea. Rev.*, **86**, 457–466.

Townsend, A. A., 1956: *The structure of turbulent shear flow.* Cambridge, Cambridge University Press, 315 pp.

Turner, J. S., 1957: Buoyant vortex rings. *Proc. Roy. Soc.*, Ser. A, **239**, 61–75.

——, 1960: A comparison between vortex rings and vortex pairs. *J. fluid Mech.*, **7**, 419–432.

Woodward, B., 1959: The motion in and around isolated thermals. *Quart. J. R. meteor. Soc.*, **86**, 144–151.